Simultaneous Synchrotron X-ray Diffraction and Stress−Strain or Stress−Relaxation Experiments for the Study of Parallel and Perpendicular Orientation in a Liquid Crystalline Polymer

Juan P. Fernández-Blázquez, Antonio Bello, María L. Cerrada, and Ernesto Pérez*

Instituto de Ciencia y Tecnología de Polímeros (CSIC), Juan de la Cierva 3, 28006-Madrid (Spain)

Received July 3, 2007; Revised Manuscript Received October 11, 2007

ABSTRACT: The orientational behavior of a thermotropic polybibenzoate exhibiting a low-ordered smectic mesophase has been studied by real-time simultaneous synchrotron X-ray diffraction and stress−strain or stress−relaxation experiments. It follows from the stress−strain test (conducted at 105 °C and with a nominal strain rate of 3.33 min^{-1}) that during the initial elastic region and around the yielding point, exclusively anomalous perpendicular orientation is obtained, with the molecular axes perpendicular to the uniaxial deformation direction. However, at the end of the necking region and the beginning of the strain-hardening process, parallel orientation begins to be obtained, and its intensity increases with the strain hardening. The intensity and spacing of the smectic spots and the layer order parameters for the two kinds of orientation have been obtained from the corresponding radial and azimuthal integrations of the photographs. One interesting finding is the observation of a 4% maximum expansion of the smectic spacing for the parallel orientation. In the subsequent stress−relaxation experiment, very little influence has been found on the smectic regions showing perpendicular orientation, but a progressively better parallel ordering is observed with an intensity increase by a factor of 3.2, with a very important increase of the order parameter, and with a simultaneous decrease of the smectic layer spacing. This decrease shows a perfect match with the stress−relaxation curve, in such a way that the two magnitudes, stress and smectic spacing, can be fitted to stretched exponential KWW functions with rather similar parameters.

Introduction

Liquid-crystalline polymers, LCPs, have found one of the most interesting applications in the production of high modulus fibers, taking advantage of the inherent anisotropy of the constituent molecular chains. Moreover, their particular hierarchical structure, with different levels of organization, and correlation of this structure with the final properties also form an attractive aspect of these systems.[1,2]

It has been reported that some LCPs with smectic or nematic mesophases may exhibit, under particular circumstances of uniaxial stretching or shear deformation, a kind of anomalous orientation where the chain axes are perpendicular to the stretching direction.[3−14] As a consequence, the best mechanical properties in such systems are found in the direction normal to the fiber,[6] so that new prospects are envisaged from this particular behavior.

Focusing the attention on the orientation attained by uniaxial stretching, it has been reported that the strain rate and the deformation temperature are very important parameters for the obtainment of either parallel or perpendicular orientation. Unfortunately, those studies were not performed in real-time experiments, since the fibers were stretched under particular conditions and then the kind of orientation was analyzed from the corresponding X-ray fiber photographs acquired in a conventional diffractometer.

However, taking advantage of the extremely high intensity of synchrotron radiation, very short acquisition times can be used, so that the corresponding experiments can be performed under real time conditions, simultaneously to the registration, for instance, of the stress−strain measurements, if the adequate setup is implemented in the synchrotron beamline.

* Corresponding author. E-mail: ernestop@ictp.csic.es.

Moreover, the prediction and understanding of the stress relaxation behavior of polymer systems in general is also of particular importance, because it may provide valuable information about the molecular mechanisms affecting the macroscopic properties of the material. Besides, a very rich phenomenology is underlying the analysis of the stress relaxation behavior of polymers.

The purpose of this work is to analyze the orientational behavior of a smectic liquid-crystalline polybibenzoate that is able to exhibit either parallel or perpendicular orientation. Real-time simultaneous synchrotron X-ray diffraction and stress−strain or stress−relaxation experiments have been performed and the corresponding variations of the intensity and spacing of the smectic spots, and of the order parameters for the two kinds of orientation, are determined from the radial and azimuthal integrations of the photographs.

Experimental Section

The polymer has been synthesized by melt transesterification of diethyl *p,p′*-bibenzoate with 2-methyl-1,3-propanediol, using isopropyl titanate as catalyst. It was purified by precipitating into methanol a chloroform solution. The polymer, named as PB32, has the following structural unit:

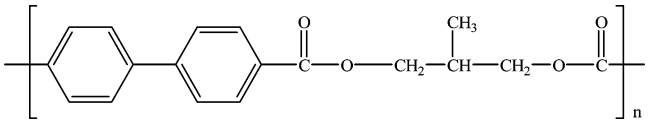

Size-exclusion chromatography data were obtained using a Waters 150C gel permeation chromatograph, equipped with two detectors: the conventional refractive index concentration detector and a viscometer Retrofit GPC 150R from Viscotek Co. After a universal calibration (from measurements in different

10.1021/ma071474m CCC: $40.75
Published on Web 12/19/2007

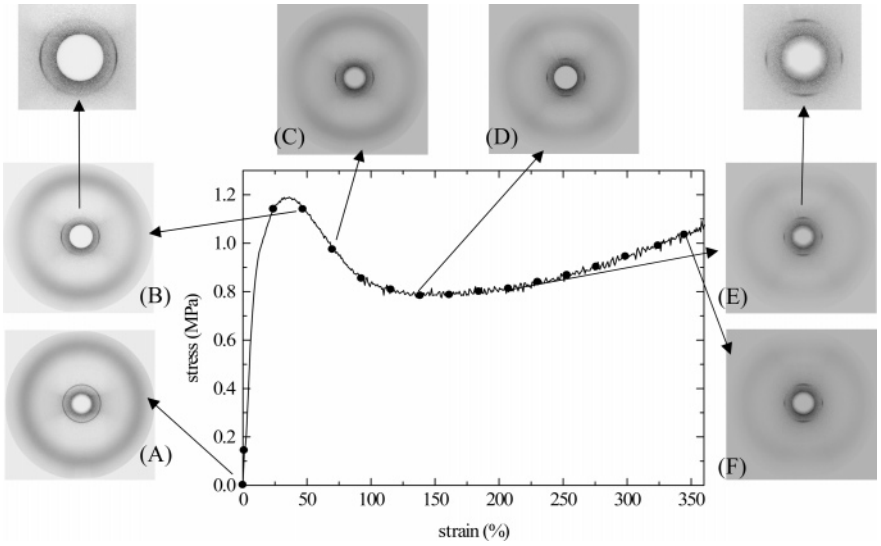

Figure 1. Stress−strain curve corresponding to PB32 stretched at 105 °C and 3.33 min^{-1}, and simultaneous 2D X-ray photographs acquired at selected times. The full points over the curve represent the strains where photographs were actually taken. The magnification of the smectic layer peak region is also presented for photographs B and E. Fiber direction: vertical.

polystyrene standards, using chloroform as eluent at 25 °C), the obtained molecular weight values are as follows: M_w = 15 900 and M_n = 7600, with an intrinsic viscosity of 0.41 dL/g.

A film of the polymer was obtained by compression molding in a Collin press between hot plates (200 °C) at a pressure of 1.5 MPa, and subsequently cooling down to room temperature between water-cooled plates in the press. Dumbbell shaped specimens with gauge dimensions of 9 mm in length and 3.5 mm in width were punched out from the polymer sheet with a standardized die. Thickness of specimens was around 0.6 mm.

Differential scanning calorimetric measurements were carried out with a Perkin-Elmer DSC7 calorimeter connected to a cooling system, at a heating rate of 20 °C/min.

A Minimat 2000 dynamometer was vertically mounted on a bench, provided with XYZ motors, in beamline BM16 at the ESRF (Grenoble, France). The original glass windows of the Minimat furnace were replaced by Kapton ones, transparent to X-rays. The movement of the lower clamp of the Minimat during the stress−strain experiments is compensated by the corresponding movement of the Z motor. Tensile testing was carried out at 105 °C and a crosshead speed of 30 mm/min, up to a final strain of 360%. After that, and with no discontinuity, a relaxation experiment was programmed, registering the nominal stress at constant strain as a function of time (at the same temperature of 105 °C).

The stress−strain or stress−relaxation curves are registered by the Minimat computer, while the corresponding X-ray fiber photographs were acquired simultaneously at the desired times, by using a MARCCD detector located at 288 mm from the polymer sample. An acquisition time of 0.5 s was used. The X-ray beam was monochromatized at the selenium edge (λ = 0.0978 nm). The 2D X-ray diffractograms were processed using the FIT2D program of Dr. A. Hammersley of ESRF. The profiles were normalized to the primary beam intensity, and the background from an empty sample was subtracted.

The radial integrations of the photographs were performed in four slices of 90°, with 45° above and below the equator, and at the left and the right of the meridian. Since the stretching direction is vertical, the average of the two meridional slices will account for the regular parallel orientation, while the two equatorial ones, for the anomalous perpendicular orientation. In both cases, the eventual isotropic intensity is also included. The corresponding profiles represent relative intensity units as a function of the scattering vector, $q = 2\pi/d = 4\pi(\sin\theta)/\lambda$.

The azimuthal integrations were performed in a narrow range of scattering vectors (from q = 3.9 to 5.2 nm^{-1}) around the smectic layer diffraction, and taking as origin of the azimuthal angle the stretching direction (the upper part of the meridian). The order parameters were obtained from these azimuthal profiles after subtraction of a flat baseline accounting of the remaining isotropic intensity in the sample and for the possible incoherent scattering. Moreover, since the noise has also a very important effect on the order parameter, the profiles were smoothed prior to the corresponding calculations (see below).

Results and Discussion

Thermal Behavior. The DSC melting curve corresponding to polymer PB32 shows a glass transition, centered at around 65 °C, followed by an endothermic peak at 173 °C, comprising an enthalpy of 16 J/g. This low enthalpy is typical for the isotropization of low ordered smectic mesophases in polybibenzoates. In fact, the X-ray results (see below) will confirm the presence of this smectic mesophase, so that the endotherm corresponds to the isotropization of such mesophase. The kind of mesophase will be deduced from the corresponding fiber photographs.

No further transformation of this mesophase into another phase of higher order has been detected in PB32. It seems that the presence of the lateral methyl substituent in the spacer prevents the development of higher states of order.

Stress−Strain Experiments. The stress−strain results for the experiment of deformation of PB32 at 105 °C and a nominal deformation rate of 3.33 min^{-1} (crosshead speed of 30 mm/min) are shown in Figure 1, where some characteristic 2D X-ray diffractograms are also presented. The diffractogram corresponding to the initial isotropic sample, before stretching, is shown in photograph A of Figure 1. Two diffractions are observed: a sharp one, at lower angles, corresponding to a spacing of 1.382 nm, and a broad amorphous-like halo, at high angles. This pattern is characteristic of a low ordered smectic structure, with a regular disposition of the smectic planes, spaced by 1.382 nm, and the absence of lateral order inside the smectic planes.

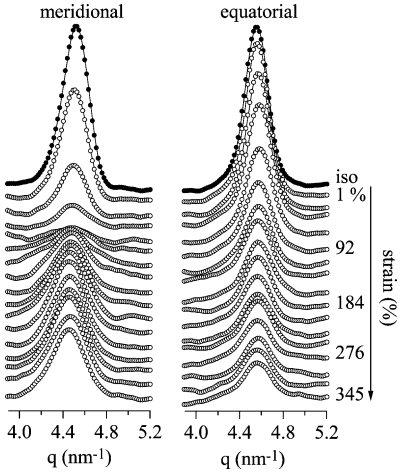

Figure 2. Results for the radial integration, in the region of the smectic layer spacing, of the X-ray photographs obtained during the stress−strain experiment in Figure 1, for the meridional and equatorial slices.

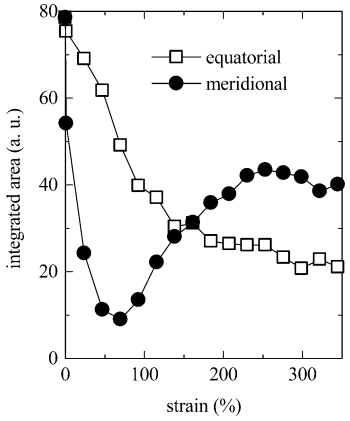

Figure 3. Variation with strain of the intensity of the smectic peaks corresponding to meridional (circles) and equatorial (squares) components, compared to the isotropic intensity.

Although we are dealing with a low-ordered smectic mesophase, the stress−strain curve in Figure 1 resembles that for a semicrystalline polymer (except for the rather low values of the stress), and three regions can be observed: an initial elastic region, a necking zone and a final strain-hardening region. A well characteristic and different orientational behavior is exhibited in these three regions, as deduced from the corresponding X-ray fiber photographs. Thus, the initial elastic region exhibits a Young modulus of around 12 MPa, a rather low value, as corresponds to a low-ordered smectic mesophase. The orientational behavior in this region and around the yielding point is characterized, as expected, by the loss of the initial isotropic X-ray diffractogram (photograph A in Figure 1) and a progressive increase of the order parameter, as deduced from the corresponding azimuthal integration of the photographs (see below). However, it is interesting to note that the orientation achieved is anomalous: a perpendicular orientation is observed, since the smectic arcs (or spots) are located on the equator (see photograph B and its amplification in Figure 1), indicating that the molecular axes are preferentially aligned perpendicular to the stretching direction.

In the necking region, which shows a yielding point at a strain of 35% and a stress of 1.19 MPa, the order parameter continues increasing progressively, and it is observed that 100% of perpendicular orientation is achieved in photograph C (as deduced from Figure 2, this photograph corresponds to a strain of 70%).

On the other hand, photograph C indicates that while the smectic peak intensity is concentrated on the equator, the outer amorphous like halo is split into two maxima, at the left and the right of the meridian. This pattern is characteristic of a mesophase with consecutive mesogens arranged in an alternating antiparallel fashion (SmC_{alt} mesophase), typical for polybibenzoates with odd spacers.[10,11] Evidently, since we are dealing with anomalous perpendicular orientation, this pattern is shifted by 90° in relation to the usual SmC_{alt} diffractogram showing parallel orientation.

Even more interesting is the orientational behavior in the third region, where strain-hardening is observed. Thus, photographs E and F in Figure 1 show an increasing intensity of smectic peak in the meridian, indicating that during this strain-hardening the most relevant feature is the obtainment of increasingly higher amounts of parallel, normal, orientation.

Detailed and quantitative information can be obtained from both the radial and azimuthal integration of the 2D X-ray photographs, which were acquired at the positions of the full points represented in Figure 1. The corresponding radial integrations, in the region of the smectic layer spacing, are presented in Figure 2 for both the meridional and equatorial slices, compared to the profile of the isotropic sample. The left diagram of Figure 2 indicates that the smectic peak intensity in the meridional slices (which includes the parallel orientation) decreases very rapidly and vanishes after a few frames, although some of the intensity is recovered later on.

Regarding the perpendicular orientation, it can be observed in the diagram at the right of Figure 2 that the intensity in the equatorial slices decreases more or less smoothly and continuously.

The evolution of the meridional and equatorial intensities is shown in Figure 3, compared to the initial intensities corresponding to the first photograph (isotropic sample). The initial rapid decrease of the meridional intensity and its later recovery is clearly observed, together with the smooth decrease of the equatorial area.

These values of total integrated area include, evidently, both the intensity of the oriented regions and a certain amount of nonoriented isotropic regions. The relative fraction of oriented sample will be estimated below, from the azimuthal integration profiles, and it is found that no parallel orientation is obtained for strains below around 120%. Therefore, the first points for the meridional spacing reflect exclusively the evolution of the isotropic regions.

Another important information that can be deduced from the diagrams in Figure 2 is the location of the peaks, inversely related to the smectic layer spacing. The corresponding results are presented in Figure 4. The upper diagram shows the evolution of the smectic spacing, *d*, in the meridian (including the parallel orientation), compared with the stress−strain curve. A certain qualitative resemblance between the behavior of the smectic spacing and the stress−strain curve is found.

It follows, therefore, that there is a certain relation between the macroscopic strain and the expansion of the smectic layer spacing in the parallel direction. However, the yielding point in the stress−strain curve corresponds to a macroscopic strain of 35%, while the maximum expansion of the parallel smectic spacing is only around 4%. Consequently, the deformation at this microscopic scale is strongly non-affine. This behavior can be expected when considering that at this microscopic level there are severe geometrical constraints, imposed by bond lengths, bond angles and hindrance potentials.[18] More or less affine or pseudo-affine behaviors are expected at higher scales: for instance, for the deformation of the radius of gyration in

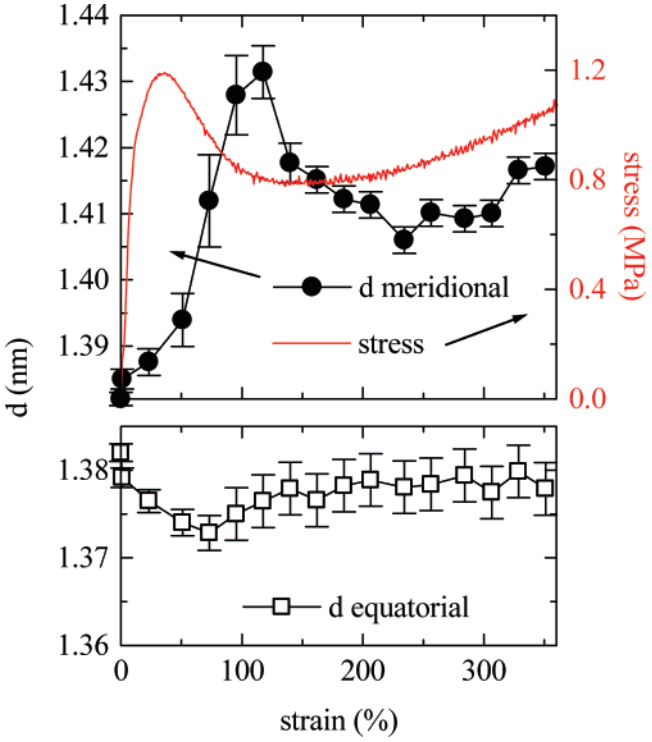

Figure 4. Variation with strain of the smectic spacing corresponding to the equatorial (lower frame) and meridional (upper frame) peaks. The stress−strain curve is also shown in the upper frame.

amorphous polymers[18−20] or for the spherulitic deformation in semicrystalline polymers.[21−23]

In the particular case of mesomorphic polymers, previous reports[24,25] have shown that more than a single conformation, compatible with the low requirements of the mesophase order, could intervene in the formation of the smectic layers. In the case of parallel orientation, therefore, uniaxial stretching is expected to favor those more extended conformations, thus explaining the increase of the spacing in the direction of stretching.

The variation of the smectic layer spacing in the perpendicular direction is shown in the lower part of Figure 4. Again, a certain relation with the stress−strain curve is obtained, although there are two obvious differences: first, we get now a contraction of the smectic spacing; second, this contraction is rather small: it is almost inside the experimental error and amounts to a maximum of only 0.7% in relation to the isotropic value.

Evidently, the fiber after stretching presents a clear macroscopic contraction in the direction perpendicular to the stretching. In fact, the width of the specimen changes from an initial value of 3.5 mm to 1.25 mm at the end of the experiment. This macroscopic contraction is somehow reflected on the perpendicular smectic spacing, although in a very much lower extent.

Additional information has been obtained from the azimuthal integration of the X-ray fiber photographs. The corresponding results in the region of the smectic layer spacing are shown in Figure 5, as a function of the strain. Initially, a flat line is obtained, as corresponds to an isotropic sample. Later on, the appearance of perpendicular and parallel orientation, with the smectic diffractions concentrated on the equator and on the meridian, respectively, is characterized by the observation of maxima at azimuthal angles of 0 and 180° for the parallel orientation, and at 90 and 270° for the perpendicular one.

In principle, the amount of each kind of orientation can be determined from these profiles by integrating the corresponding peaks, after subtraction of the flat baseline (see Experimental

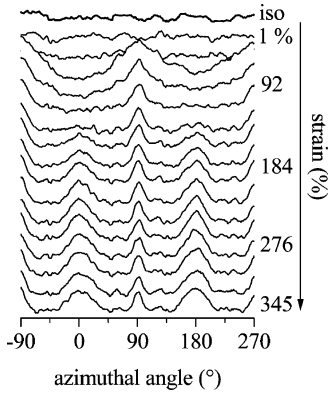

Figure 5. Results for the azimuthal integration, in the region of the smectic layer spacing, of the X-ray photographs obtained during the stress−strain experiment in Figure 1.

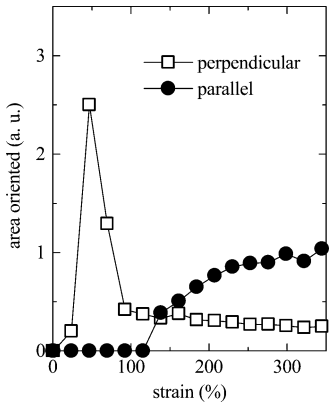

Figure 6. Estimated areas of perpendicular (squares) and parallel (circles) orientation as a function of strain.

Part). The results are plotted in Figure 6. However, since the structure factors of the two kinds of orientation may be different, these intensities may have a different proportionality factor in relation to the actual amount of polymer segments exhibiting each kind of orientation.

Nevertheless, from all the previous results it follows that in the initial stages, for experimental strains smaller than around 120%, the great majority (or the totality) of the oriented regions exhibit perpendicular, anomalous, orientation. On the contrary, for higher strains, and coinciding with the strain-hardening process, the parallel orientation shows up and increases smoothly, in such a way that its intensity becomes predominant above a strain of around 150%, as observed in Figure 6.

From the results in Figure 5, the order parameter can be also determined. The average degree of orientation of the smectic layers with respect to the stretching direction can be represented by the order parameter, which can be related to the spherical harmonics of the probability distribution,[1] similarly to the case of the Hermans orientation function for semicrystalline polymers. It is usual to neglect the higher harmonics, and thus the order parameter, S, is equivalent to the second harmonic, P_2, according to

$$\langle P_2 \rangle = (3\langle \cos^2 \alpha \rangle - 1)/2 \qquad (1)$$

where α is the azimuthal angle in relation to the meridian, i.e., the stretching direction. The average in the right-hand of eq 1 can be determined from the intensity distribution, $I(\alpha)$, as follows:[26,27]

$$\langle \cos^2\alpha \rangle = \frac{\int_0^{\pi/2} I(\alpha) \cos^2\alpha |\sin\alpha| \, d\alpha}{\int_0^{\pi/2} I(\alpha) |\sin\alpha| \, d\alpha} \quad (2)$$

Therefore, a perfectly uniaxially oriented sample will have $S = 1$, while a completely isotropic sample is characterized by $S = 0$.

In principle, there is only a single axis (the stretching direction) about which uniaxial symmetry may be assumed, and, for a certain 2D-photograph, a single overall order parameter is deduced from eqs 1 and 2. However, for this particular case where the orientation is exclusively observed around the meridian or the equator, and not at intermediate angles, the use of the overall order parameter is rather nonintuitive for extracting conclusions about the independent evolution of the parallel and perpendicular orientations. As was pointed out before,[26] the assignment of the axes or directors for the oriented units is the first step in describing the development of orientation and, in the case of polymers, the draw direction is the usual choice, although the direction of the chain axis is of major interest. Thus, we have estimated the order parameter independently for the parallel and perpendicular orientation by choosing in both cases the molecular axis direction as reference for the azimuthal angle in eq 2. With this choice, the corresponding order parameters will reflect the degree of layer orientation independently for each kind of orientation.

Therefore, the azimuthal angle depicted in Figure 5 is the one used for the order parameter of the parallel orientation, while it has been shifted by 90° for the perpendicular one. Evidently, the integrations in eq 2, extending in principle to 90°, have been truncated when the two orientations are present, considering only the corresponding particular orientation.

The results for the two independent order parameters are presented in Figure 7. It can be observed that the order parameter for the perpendicular orientation increases rather steeply from 0 to 0.95 (this corresponding to a strain of 115%) and later there is a much slower increase, up to a value of 0.97 at the end of the experiment.

On the other hand, the parallel component is clearly observed only above 130% strain, and it shows initially a roughly constant value of around 0.84 for the order parameter. For strains higher than around 250%, it decreases down to a final value of 0.74. This decrease seems to be related to the maximum slope in the stress−strain curve due to strain hardening.

Anyway, the order parameters corresponding to the parallel orientation are significantly lower than those for the perpendicular component, as can be anticipated just by comparing the widths of the corresponding peaks for the azimuthal integration in Figure 5: the peaks for the perpendicular orientation are considerably narrower.

A model for the two kinds of orientation, based on the hierarchical structure of liquid-crystalline polymers,[2,28−30] has been proposed.[3] In that model, the initial structure of our smectic polymer can be envisaged as composed of domains randomly oriented but with a rather uniform order parameter inside the domains. If it is assumed that the dimensions of the domains in the lateral directions are considerably larger than in the direction of the molecular axis, it seems reasonable to expect that in the case of low strain rates and/or high deformation temperatures, these domains will be able to slide through the disclinations and reorient in relation to the direction of deformation, ending with the largest dimension oriented with the deformation, so that the molecular axes are perpendicular to the stretching direction: *anomalous orientation*.

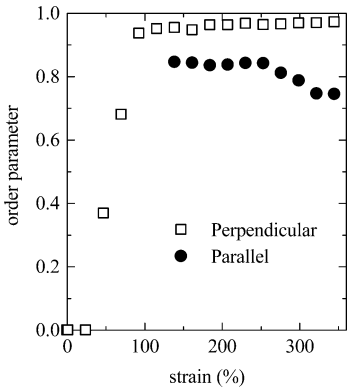

Figure 7. Variation with strain of the layer order parameter corresponding to parallel (circles) and perpendicular orientation (squares) for the stress−strain experiment.

On the contrary, in the case of high strain rates and/or low temperatures, the domains will not be able to follow the deformation, and, presumably, they will broke apart and reorganize into some kind of fibrillar structure, ending with the molecular axes parallel to the direction of deformation: *normal orientation*.

Of these two kinds of orientation pathways, the one leading to perpendicular alignment is rather singular in the field of polymers. It has been found in a few liquid-crystalline polymers, as in the present case, and also in block copolymers.[31] On the contrary, the model for parallel orientation is similar to that proposed for the deformation of semicrystalline polymers,[32,33] where the initial lamellar crystals, through chain tilting, slip and breaking off, and subsequent re-formation of domains, lead to a fiber formation, oriented along the stretching direction.

In the present case, it follows from the previous results that exclusively perpendicular orientation is achieved during the initial stages of deformation, and only after necking the parallel orientation shows up, coexisting with other regions exhibiting perpendicular orientation, and, interestingly, the order parameter in the perpendicular domains is significantly higher than that in the regions with parallel orientation.

Evidently, and as was shown before in the non-real-time experiments,[3] the proportions of the two kinds of orientations will depend very much on the stretching conditions (temperature and rate of deformation, principally).

Relaxation Experiments. The dynamometer was programmed to register a stress−relaxation ramp at the end of the previous stress−strain experiment, with no discontinuity (and at the same temperature of 105 °C). Simultaneously, 2D X-ray photographs were acquired. To our knowledge, there are no such simultaneous studies in the literature.

The stress−relaxation curve (following the stress−strain experiment depicted in Figure 1), is shown in Figure 8, together with the corresponding 2D X-ray fiber photographs at selected relaxation times. An important increase of the intensity corresponding to parallel orientation is observed, since the smectic spots on the meridian are clearly more intense for the higher relaxation times.

As before, all the X-ray photographs (acquired at the times marked by the full points in Figure 8) have been integrated both radially and azimuthally. The radial integrations, in the region of the smectic layer spacing, are presented in Figure 9. It is observed that the integral peaks on the equator (perpendicular orientation) keep approximately constant in both intensity and position. On the contrary, the left diagram of Figure 9 indicates that the meridional peaks show a very important intensity increase and also a small shift.

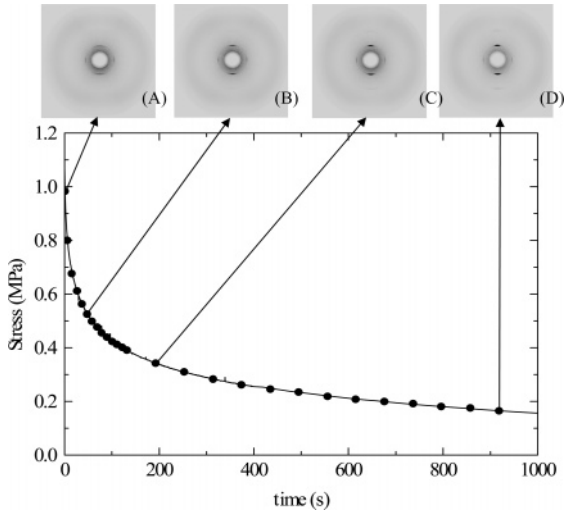

Figure 8. Stress−relaxation curve corresponding to PB32 after its stretching at 105 °C and 3.33 min^{-1} up to a strain of 360% (Figure 1). The simultaneously acquired 2D X-ray photographs at the selected indicated times are also shown. The full points over the curve represent the times where photographs were actually taken. Fiber direction: vertical.

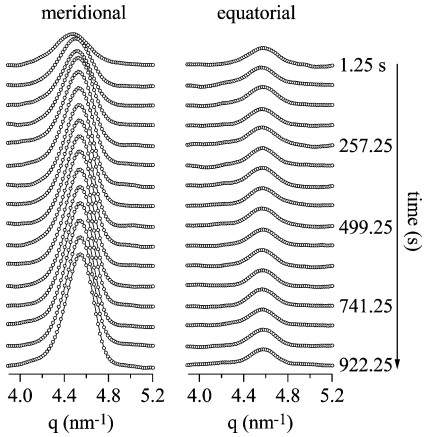

Figure 9. Results for the radial integration, in the region of the smectic layer spacing, of the X-ray photographs obtained during the stress−relaxation experiment in Figure 8, for the meridional and equatorial slices. For simplicity, not all profiles are shown. The intensity scale in this figure is 2 times smaller than in Figure 2.

Therefore, the most relevant feature during stress relaxation corresponds to an increasingly better parallel ordering, arising either from nonaligned molecules or from the perfection of the domains showing such parallel orientation. It is clear that the increase on the "parallel" intensity is not arising, as it could be expected, from a corresponding decrease in the "perpendicular" one.

Rather interesting is also the variation of the smectic spacing corresponding to both types of orientation. Thus, Figure 10 shows a rather small decrease (practically inside the experimental error) of the perpendicular spacing. However, the parallel spacing exhibits a very important decrease, pointing to an asymptotic values of around 1.370 nm, somewhat smaller than the initial isotropic value (see Figure 4). It has to be considered that the regions exhibiting parallel ordering have been obtained by a re-formation of the initial domains, so that their "equilibrium" spacing may differ from the isotropic one.

Interestingly, the continuous curve plotted in Figure 10 is the *experimental* stress−relaxation curve registered by the dynamometer. It can be observed that by appropriate selection of the two Y-axis scales (stress and smectic spacing), the stress−

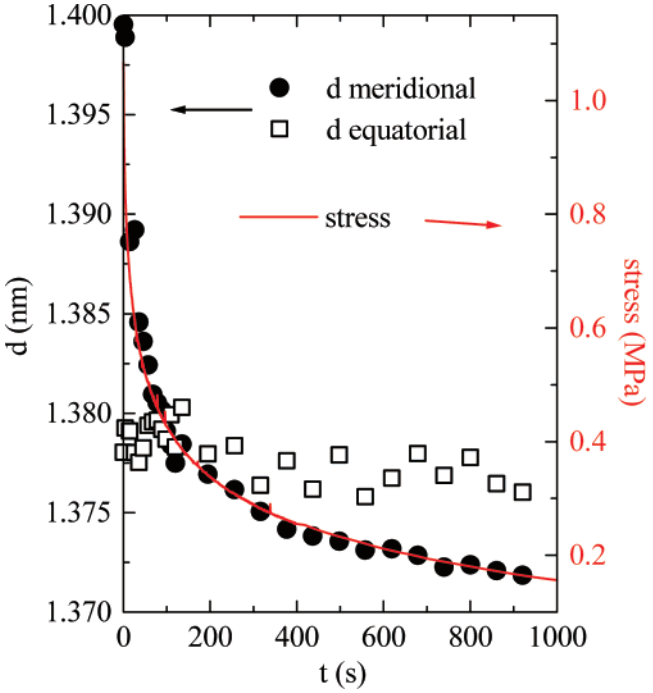

Figure 10. Variation with the relaxation time of the smectic spacing corresponding to equatorial (squares) and meridional (circles) peaks. The stress−relaxation *experimental* curve is also shown.

relaxation curve appears as if it were just the fitting to the experimental variation of the parallel smectic spacing. It seems, therefore, that the phenomenology underlying the two variations (stress and spacing) with time is rather similar or exactly the same.

Focusing the attention on the stress−relaxation curve itself, it has been reported in several polymer systems that relaxation phenomena obey a stretched exponential decay behavior[34−36] which can be described by a modification of the Kohlrausch−Williams−Watts (KWW) equation[37,38] in such a way that the stress at a certain time, $\sigma(t)$, can be described as

$$\sigma(t) = (\sigma_0 - \sigma_\infty) \exp(-t/\tau)^\beta \qquad (3)$$

where σ_0 is the initial stress at zero time, σ_∞ is the asymptotic value at very long times, τ is the characteristic relaxation time, and the parameter β is a measure of the nonexponentiallity of the relaxation, usually ascribed to a superposition of different processes, with the subsequent distribution of relaxation times. Thus, the parameter β is found to be inversely related to the width of that distribution.

The stress−relaxation curve in Figure 8 can be successfully fitted to eq 3 with the following parameters: $\sigma_0 = 1.20 \pm 0.05$ MPa; $\sigma_\infty = 0.02 \pm 0.05$ MPa; $\tau = 85 \pm 5$ s; $\beta = 0.31 \pm 0.02$. The relatively low value of β seems to indicate a broad distribution of relaxation times. On the other hand, an asymptotic value practically zero is obtained for σ_∞, thus indicating a complete relaxation of the stress at infinite times.

Rather similar values for τ and β are obtained when fitting the experimental results for the parallel smectic spacing as a function of the relaxation time to a stretched exponential function similar to that in eq 3: just replacing stress values for d spacing. The corresponding best fitting parameters are the following: $d_0 = 1.402 \pm 0.002$ nm; $d_\infty = 1.368 \pm 0.002$ nm; $\tau = 80 \pm 5$ s; $\beta = 0.31 \pm 0.02$. The similarity of the τ and β parameters obtained in the fitting of stress or spacing is remarkable, as could be anticipated from the observation of Figure 10.

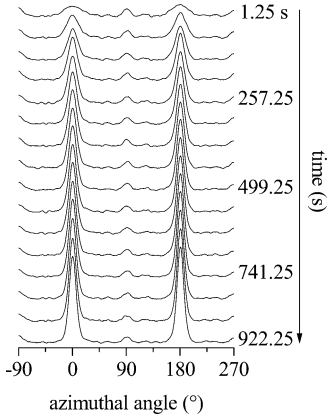

Figure 11. Results for the azimuthal integration, in the region of the smectic layer spacing, of the X-ray photographs obtained during the stress−relaxation experiment in Figure 8. For simplicity, not all profiles are shown. The intensity scale in this figure is 2 times smaller than in Figure 5.

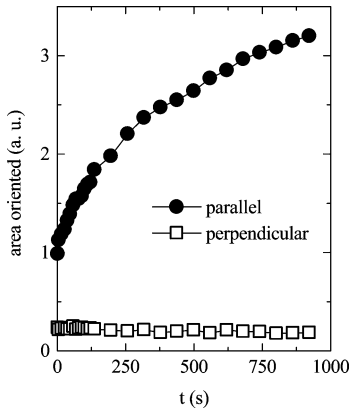

Figure 12. Estimated areas of perpendicular (squares) and parallel (circles) orientation as a function of the relaxation time.

A final analysis of these relaxation experiments corresponds to the azimuthal integration of the X-ray fiber photographs. The results are shown in Figure 11. It can be observed that the peaks at azimuthal angles of 90 and 270°, corresponding to the smectic regions exhibiting perpendicular orientation, keep practically the same in both intensity and width. However, those at 0 and 180°, i.e., those for the parallel orientation, increase very much in intensity, and the width diminishes clearly as the relaxation time increases.

As before, the relative proportions of regions exhibiting each kind of orientation has been determined from the azimuthal profiles. The results are shown in Figure 12. It can be observed that while the perpendicular orientation decreases somewhat, the parallel one increases by a factor of 3.2. However, as pointed out before, these values may not represent the true fractions of sample exhibiting each kind of orientation, since the structure factors may be different. Anyway, it seems evident that the increase of the parallel intensity is not at the expenses of the perpendicular one

Finally, the values for the two independent layer order parameters, deduced from the data in Figure 11 by applying eqs 1 and 2, are shown in Figure 13. It can be observed that the perpendicular component exhibits a fairly constant value of 0.97, while the order parameter for the parallel orientation presents a continuous, close to logarithmic, increase up to a final value of around 0.97. Thus, the order parameters for the two kinds of orientations are practically the same at the end of the experiment.

Therefore, the relaxation of stresses in the fiber of PB32 stretched at 105 °C up to a strain of 360% exerts very little

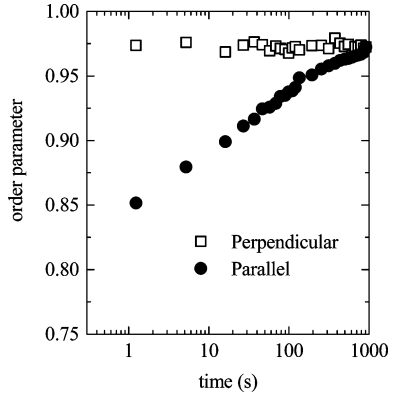

Figure 13. Variation with the relaxation time of the layer order parameter corresponding to parallel (circles) and perpendicular orientation (squares) for the stress−relaxation experiment.

influence on the smectic regions showing perpendicular, anomalous, orientation, since the total intensity, the smectic spacing and the order parameter are practically unchanged. Quite different is the behavior of the regions where parallel orientation is exhibited, and it seems that one of the most important mechanisms of stress relaxation is the perfection of such parallel orientation, with a very important increase in the order parameter, and with a simultaneous decrease of the smectic layer spacing.

Conclusions

The real-time simultaneous synchrotron X-ray diffraction and stress−strain experiments, performed in a sample of the thermotropic polybibenzoate PB32 at 105 °C and with a nominal strain rate of 3.33 min^{-1}, indicate that during the initial elastic region and around the yielding point exclusively anomalous perpendicular orientation is obtained, with the molecular axes perpendicular to the uniaxial deformation direction. However, at the end of the necking region and the beginning of the strain-hardening process, parallel orientation begins to be obtained, and its intensity increases with the strain hardening.

The intensity and spacing of the smectic spots, and the layer order parameters for the two kinds of orientation, have been obtained from the corresponding radial and azimuthal integrations of the photographs. One interesting finding is the observation of a 4% maximum expansion of the smectic spacing for the parallel orientation and a 0.7% contraction of the perpendicular one.

In the subsequent stress−relaxation experiment, very little influence has been found on the smectic regions showing perpendicular orientation, but a progressively better parallel ordering is observed with a an intensity increase by a factor of 3.2, with a very important increase of the order parameter, and with a simultaneous decrease of the smectic layer spacing. This decrease shows a perfect match with the stress−relaxation curve, in such a way that the two magnitudes, stress and smectic spacing, can be fitted to stretched exponential KWW functions with rather similar parameters. It seems that one of the most important mechanisms of stress relaxation is the perfection of such parallel orientation.

Acknowledgment. This work was funded by the Ministerio de Educación y Ciencia, MEC (Project MAT2004-06999-C02-01). The synchrotron work was also supported by MEC through specific grants for the access to the CRG beamline BM16 of the ESRF. The inestimable help of all the beamline personnel is also gratefully acknowledged.

References and Notes

(1) Donald, A. M.; Windle, A. H. *Liquid Crystalline Polymers*; Cahn, R. W., Davis, E. A., Ward, I. M., Eds.; Cambridge University Press: Cambridge, U.K., 1992.
(2) MacDonald, W. A. In *Liquid Crystal Polymers: From Structures to Applications*; Elsevier: New York, 1992; Chapter 8, p 407.
(3) Fernández-Blázquez, J. P.; Bello, A.; Pérez, E. *Macromolecules* **2007**, *40*, 000.
(4) Bello, P.; Bello, A.; Lorenzo, V. *Polymer* **2001**, *42*, 4449.
(5) Bello, P.; Bello, A.; Riande, E.; Heaton, N. *Macromolecules* **2001**, *34*, 181.
(6) Martínez-Gómez, A.; Pereña, J. M.; Lorenzo, V.; Bello, A.; Pérez, E. *Macromolecules* **2003**, *36*, 5798.
(7) Tokita, M.; Osada, K.; Kawauchi, S.; Watanabe, J. *Polym. J.* **1998**, *30*, 687.
(8) Tokita, M.; Tokunaga, K.; Funaoka, S.; Osada, K.; Watanabe, J. *Macromolecules* **2004**, *37*, 2527.
(9) Osada, K.; Koike, M.; Tagawa, H.; Hunaoka, S.; Tokita, M.; Watanabe, J. *Macromolecules* **2005**, *38*, 7337.
(10) Leland, M.; Wu, Z.; Chhajer, M.; Ho, R.-M.; Cheng, S. Z. D.; Keller, A.; Kricheldorf, H. R. *Macromolecules* **1997**, *30*, 5249.
(11) Ugaz, V. M.; Burghardt, W. R. *Polym. Mater. Sci. Eng.* **1998**, *79*, 369.
(12) Zhou, W.-J.; Kornfield, J. A.; Ugaz, V. M.; Burghardt, W. R.; Link, D. R.; Clark, N. A. *Macromolecules* **1999**, *32*, 5581.
(13) Romo-Uribe, A.; Windle, A. H. *Macromolecules* **1993**, *26*, 7100.
(14) Romo-Uribe, A.; Windle, A. H. *Macromolecules* **1996**, *29*, 6246.
(15) Watanabe, J.; Hayashi, M.; Nakata, Y.; Niori, T.; Tokita, M. *Prog. Polym. Sci.* **1997**, *22*, 1053.
(16) Pérez, E.; Pereña, J. M.; Benavente, R.; Bello, A. Characterization and Properties of Thermotropic Polybibenzoates. In *Handbook of Engineering Polymeric Materials*; Cheremisinoff, N. P., Ed.; Marcel Dekker: New York, 1997; Chapter 25, p 383.
(17) Pérez, E. *Liquid crystalline polymers: Polyesters of bibenzoic acid*, in *The Polymeric Materials Encyclopedia*; Salamone, J. C., Ed.; CRC Press: Boca Raton, FL, 1996; Vol. 5, p 3711.
(18) Dettenmaier, M.; Maconnachie, A.; Higgins, J. S.; Kausch, H. H.; Nguyen, T. Q. *Macromolecules* **1986**, *19*, 773.
(19) Ward, I. M. *Mechanical Properties of Solid Polymers*; Wiley-Interscience: New York, 1983.
(20) Sperling, L. H. *Polym. Eng. Sci.* **1984**, *24*, 1.
(21) Stein, R. S.; Wilkes, G. L. In *Structure and Properties of Oriented Polymers*; Ward, I. M., Ed.; Applied Science Publishers: London, 1975; Chapter 3, p 57.
(22) Lee, S. Y.; Bassett, D. C.; Olley, R. H. *Polymer* **2003**, *44*, 5961.
(23) Lin, L.; Argon, A. S. *J. Mater. Sci.* **1994**, *29*, 294.
(24) Pérez, E.; Riande, E.; Bello, A.; Benavente, R.; Pereña, J. M. *Macromolecules* **1992**, *25*, 605.
(25) Bello, A.; Riande, E.; Pérez, E.; Marugán, M. M.; Pereña, J. M. *Macromolecules* **1993**, *26*, 1072.
(26) Windle, A. H. In *Developments in Oriented Polymers-1*; Ward, I. M., Ed.; Applied Science Publishers: London and New Jersey, 1982; Chapter 1, p 1.
(27) Baltá-Calleja, F. J.; Vonk, C. G. *X-Ray Scattering of Synthetic Polymers*; Elsevier: Amsterdam, 1989.
(28) Sawyer, L. C.; Jaffe, M. *J. Mater. Sci.* **1986**, *21*, 1897.
(29) Tsukruk, V. V.; Shilov, V. V.; Lipatov, Y. S. *Acta Polym.* **1985**, *36*, 403.
(30) Hu, Y. S.; Schiraldi, D. A.; Hiltner, A.; Baer, E. *Macromolecules* **2003**, *36*, 3606.
(31) Schmidt, G.; Richtering, W.; Lindner, P.; Alexandridis, P. *Macromolecules* **1998**, *31*, 2293.
(32) Alexander, L. E. *X-ray Diffraction Methods in Polymer Science*; Wiley: New York, 1969.
(33) Peterlin, A. *Structure of Drawn Polymers*; Technical Report AFML-TR-67-6, Dec. 1966; USAF Materials Laboratory, Wright-Patterson, AFB, Ohio, 1966.
(34) Alvarez, F.; Alegría, A.; Colmenero, J. *Phys. Rev. B.* **1991**, *44*, 7306 and references therein.
(35) Ortiz, C.; Ober, C. K.; Kramer, E. J. *Polymer* **1998**, *39*, 3713.
(36) Gurtovenko, A. A.; Gotlib, Y. Y. *J. Chem. Phys.* **2001**, *15*, 6785.
(37) Kohlrausch, F. *Pogg. Ann. Phys.* **1863**, *119*, 337.
(38) Williams, G.; Watts, D. C. *Trans. Faraday Soc.* **1970**, *66*, 80.

MA071474M